BMC Cancer

RESEARCH

Open Access

Synthetic lethality of EZH2 and DNMT Inhibition suppresses neuroblastoma proliferation via MYCN destabilization

Yuki Endo[1,2], Ryuichi P. Sugino[1], Hisanori Takenobu[1*], Kyosuke Mukae[1], Ryu Okada[1,3], Yoshitaka Shinno[1,4], Masayuki Haruta[1], Shunpei Satoh[1], Jesmin Akter[1], Naoko Hattori[5,6], Atsuko Nakazawa[7], Toshikazu Ushijima[5,8], Akira Nakagawara[9], Miki Ohira[1], Masaki Nio[2] and Takehiko Kamijo[1,3*]

Abstract

Background Enhancer of Zeste Homolog 2 (EZH2) is highly expressed in various cancers and is thought to contribute to cancer malignancy through the methylation of lysine 27 on histone H3 (H3K27). Therefore, EZH2 is an H3K27 methylase and a target of cancer epigenetic treatments. Here, we investigated the effects and functions of a small-molecule EZH2 inhibitor (EZH2i) in aggressive neuroblastoma (NB).

Methods To identify genes associated with the sensitivity to EZH2i, we classified NB cell lines into sensitive and resistant groups. EZH2i suppressed proliferation and induced cell cycle arrest in EZH2-sensitive NB cells. Transcriptome analysis revealed the de-repression of gene sets related to differentiation and cell cycle arrest. To investigate whether the gene repression in resistant cells is mediated by mechanisms other than H3K27 methylation, methylome analysis was conducted to evaluate the significance of DNA methylation. The effect of combined treatment with an EZH2 inhibitor and a DNA methylation inhibitor (DNMTi) on the growth of resistant NB cells was subsequently assessed both in vitro and in vivo, even in cells resistant to EZH2 inhibition.

Results Genes such as *TRIM63*, *VSTM2L*, *GPNMB*, and *TIMP3*, which are de-repressed by EZH2is in sensitive cells. Furthermore, the promoters of some of these genes are hypermethylated in EZH2i-resistant cells and NB tissues. Additionally, the combined treatment with EZH2i and 5-aza-dC significantly inhibited cell proliferation with MYCN destabilization at protein level, c-MYC suppression at RNA and protein level and induced a robust differentiation phenotype.

Conclusions Our study identified gene expression profiles that can distinguish the responsiveness to EZH2i in neuroblastoma, and demonstrated that DNMTi not only de-repression in gene expression but also suppress neuroblastoma growth through inhibition of MYC. These results confirm the importance of epigenetic regulation in NB biology and provide information for developing epigenetic therapies for patients with advanced NB.

Keywords EZH2, DNMT, Neuroblastoma, EPZ-6438, 5-aza-dC, MYC

*Correspondence:
Hisanori Takenobu
takenobu@saitama-pho.jp
Takehiko Kamijo
tkamijo@saitama-pho.jp

Full list of author information is available at the end of the article

Introduction

Neuroblastoma (NB) is a sympathetic nervous system-derived pediatric solid malignant tumor. High-risk NB is refractory. In contrast to that in adult cancers, somatic mutations are rare in NB and other childhood tumors [1–3]. Nevertheless, intensive genetic analyses have identified diverse genetic variations in NB, including *MYCN* amplifications, aberrant copy number alterations (including 1p loss, 11q loss, and 17q gain), single nucleotide variants (such as *ATRX* and *ALK*), chromothripsis, and *TERT* rearrangements [1, 4–6]. As epigenetic modifications involved in NB malignancy, there are changes in the DNA methylation patterns of multiple genes, including CIMP [7]. Therapeutic efficacy has been observed in several studies by suppressing epigenetic factors, such as HDAC10 and DNA methyltransferases, for the treatment of malignant NB [8, 9].

The polycomb repressor complex 2 (PRC2) molecule EZH2 plays a role in essential cellular processes, such as cell fate decision, cell cycle regulation, senescence, cell differentiation, and cancer development/progression through the epigenomic regulation of gene expression [10–13]. PRC2-mediated transcriptional control during embryogenesis is critical in the development and clinical outcomes of MYCN-driven NB [14]. Wang et al. found that EZH2 represses multiple tumor suppressors, including *CASZ1*, *CLU*, *RUNX3*, and *NGFR*, in NB cells through histone H3 methylation [15, 16]. Chen et al. reported CRISPR-Cas9 screening revealed *MYCN*-amplified NB dependency on EZH2 [17]. This study also indicate that MYCN binds to the *EZH2* promoter, thereby directly driving its expression, and EZH2 directly targets *IGFBP3*. Recently, we demonstrated the functional role of EZH2 in neuroblastoma (NB) tumorigenesis and aggressiveness, showing that *NTRK1* (*TRKA*) is a suppression target of EZH2, with its P1 and P2 promoter regions being differentially regulated by DNA methylation and EZH2-associated histone modifications [18]. Collectively, these results indicate that EZH2 plays important roles in preventing NB cell differentiation and may be a desirable target for developing novel NB therapies [17]. EZH2 inhibitors (EZH2i), such as 3-Deazaneplanocin A (DZNep), GSK-126, and Tazemetostat (EPZ-6438), have recently been developed. EPZ-6438 has been examined in detail in several preclinical studies because it is a potent, selective, and orally bioavailable small-molecule inhibitor of EZH2 enzymatic activity [19–21]. EZH2-targeting inhibitors (Tazemetostat, GSK2816126, and CPI-1205) have entered clinical trials for malignant lymphomas and advanced solid tumors [22]. Although Tazemestat is now used for treating follicular lymphoma, its effectiveness and underlying molecular mechanisms in many malignancies, particularly NB, have not yet been elucidated in detail [23].

In this study, we investigated the molecular mechanisms of action of the EZH2i EPZ-6438 by transcriptome and methylome analyses using NB cell lines and tumor samples. EZH2i-sensitive NB cells exhibit the de-repression of genes associated with terminal differentiation in various tissues. These genes are frequently silenced in EZH2i-resistant cells and NB tissues because of promoter hypermethylation. Taken together, our data demonstrate that combined treatment with EZH2 and DNMT inhibitors synergistically inhibits tumor growth both in vitro and in vivo, likely through suppressing the MYC-related proliferation pathway. Thus, combinatorial epigenetic inhibition is a novel therapeutic strategy for NB.

Materials and methods

Cell culture and reagents

Human NB cell lines were obtained from American Type Culture Collection (Manassas, VA, USA), RIKEN BRC CELL BANK (Tsukuba, Japan) and Takara Bio (Shiga, Japan). Cells were cultured in RPMI1640 or D-MEM medium (Wako, Osaka, Japan) supplemented with 10% heat-inactivated FBS and 50 µg/ml penicillin/streptomycin (Sigma-Aldrich, St. Louis, MO, USA). All cell lines were confirmed to be mycoplasma-free using a mycoplasma detection Kit (Takara Bio). EPZ-6438, GSK-126, and DZNep were purchased from Funakoshi (Tokyo, Japan). 5-aza-2′-deoxycytidine (5-aza-dC) was purchased from Tokyo Chemical Industry Company (Tokyo, Japan).

Cell proliferation assay

Cells were seeded on 96-well plates (500 per well) in 100 µl final volume. The medium was changed every 3 days. The culture was maintained under 5% CO_2, 10 µl WST-8 labeling solution (Cell counting Kit-8; DOJINDO, Kumamoto, Japan) was added, and the cells were further incubated for 1 h. The absorbance of the formazan product was measured at 450 nm using a 96-well spectrophotometric plate reader (Sunrise, TECAN, Japan) according to the manufacturer's protocol.

Half-maximal inhibitory concentration 50 calculation

The half-maximal inhibitory concentration (IC_{50}) was calculated based on the results of the WST-8 assays on day 9 using ImageJ software (Rasband, W.S., ImageJ, U. S. National Institutes of Health, Bethesda, Maryland, USA, http://imagej.nih.gov/ij/). The cells with $IC_{50} < 500$ nM and $>= 500$ nM were defined as EPZ-6438-sensitive and -resistant cells, respectively.

Colony formation assay

Cells were seeded in 6-well plates (500 cells/well) at 3 ml final volume. The medium was changed every 3 days. Colonies were stained with May–Grünwald–Giemsa and

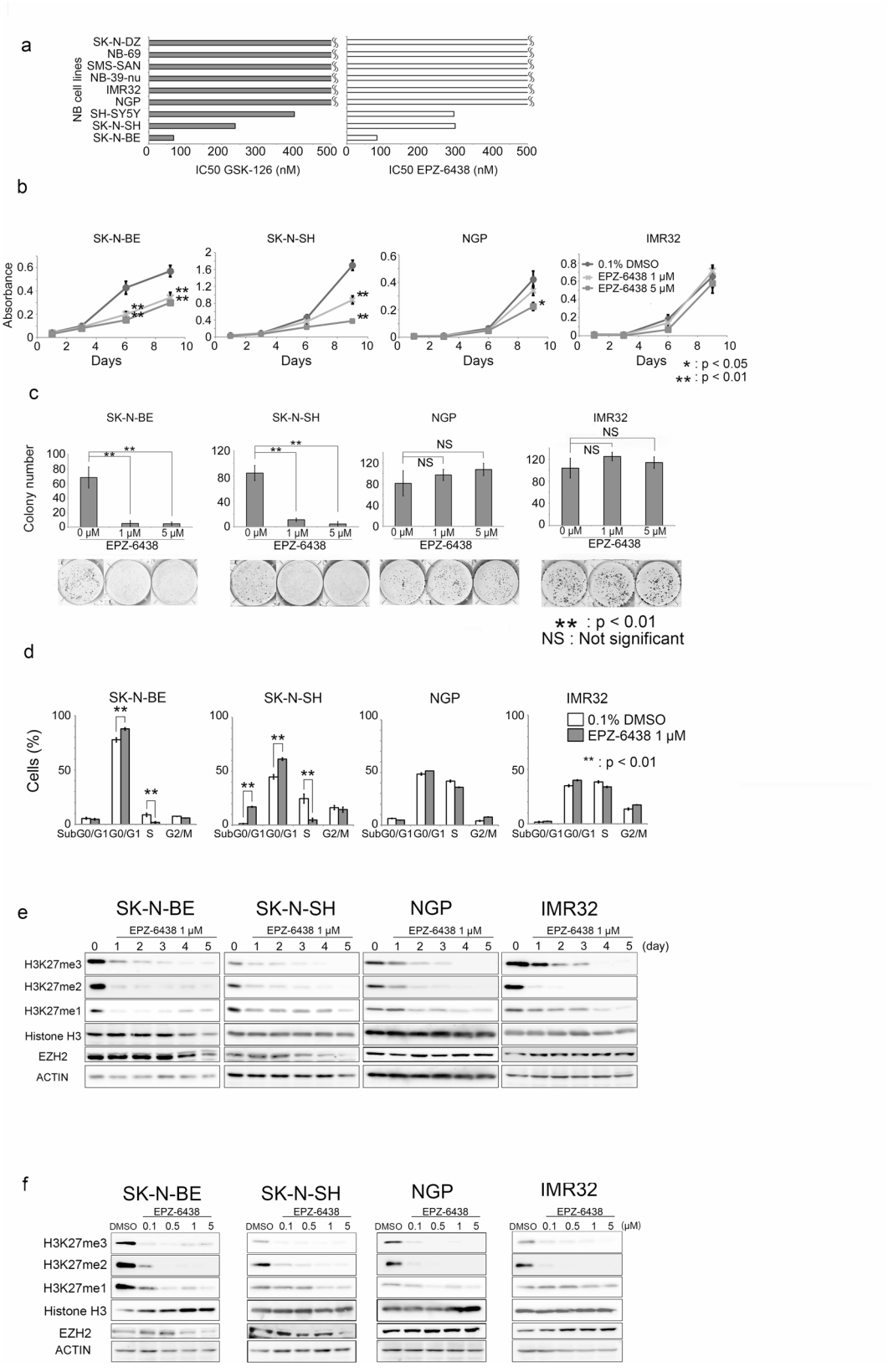

Fig. 1 (See legend on next page.)

(See figure on previous page.)

Fig. 1 EZH2 inhibitor sensitivity differences in neuroblastoma (NB) cell lines **a** GSK-126 and EPZ-6438 are selective EZH2 inhibitors (EZH2i). Nine NB cells with < 500 nM and > 500 nM half-maximal inhibitory concentration (IC_{50}) for selective EZH2i were defined as sensitive and resistant cells, respectively. NB cell proliferation was assessed using the WST assay **b**, **c** Proliferation was analyzed using WST and colony formation assays. The cells were seeded in 96- and 6-well plates for the WST and colony formation assays (500 cells per well), respectively. EPZ-6438 concentrations were 0, 1, and 5 μM. The results obtained are presented as the mean ± SD of at least three independent experiments. *P*-values were calculated using *t*-test with Bonferroni correction **d** Cell cycle analysis using FACS. NB cells were treated with 0.1% DMSO or 1 μM EPZ-6438. The cells were collected and analyzed on day 8 after treatment. The results obtained are presented as the mean ± SD of at least three independent experiments. *P*-values were calculated using Student's *t*-tests **e**, **f** Effects of EPZ-6438 were assessed by western blot analysis. The (e) upper panel shows the time-dependent effects of 1 μM EPZ-6438. (f) Lower panel shows the dose-dependent effects of EPZ-6438 on day 4 of treatment

counted using Colony Counter 1.0 software (MICROTEC CO., Japan).

Fluorescence activated cell sorting (FACS) analysis

The cell pellet was mixed with PBS containing 0.1% Triton, vortexed, and incubated at room temperature for 15 min. Propidium iodide (PI) with 2 μg/ml RNase was added to the tubes. After incubation at 37 °C for 1 h, the PI signal was measured using flow cytometry (FACS Canto II flow cytometer; BD Biosciences, San Jose, CA, USA) and cell cycle analysis was performed with FlowJo Software (BD Biosciences).

Western blotting analysis

Cells were lysed in buffer containing 5 mM EDTA, 2 mM Tris–HCl (pH 7.5), 10 mM β-glycerophosphate, 5 mg/mL aprotinin, 2 mM phenylmethylsulfonyl fluoride, 1 mM Na_3VO_4, protease inhibitor cocktail (Nacalai Tesque, Kyoto, Japan), and 1% SDS. Western blotting was performed as previously reported [18]. After being transferred to an Immobilon-P membrane (Millipore, Billerica, MA, USA), proteins were reacted with an anti-EZH2 rabbit polyclonal (Millipore Upstate 07-689), anti-trimethyl-Histone H3K27 rabbit polyclonal (Millipore 07–449), anti-dimethyl-Histone H3K27 rabbit monoclonal (Cell Signaling Technology D18C8, Danvers, MA), anti-monomethyl-Histone H3K27 mouse monoclonal (Active Motif MABI0321, Carlsbad, CA) anti-Histone H3 rabbit polyclonal (Abcam ab1791, Cambridge, United Kingdom), anti-α-Actin rabbit monoclonal (Sigma-Aldrich, 20–33, St. Louis, Missouri, USA), anti-β-Tubulin mouse monoclonal (Boehringer Ingelheim, Ingelheim am Rhein, Germany), or anti-Dnmt1 rabbit monoclonal antibody (Abcam ab188453).

Semi-quantitative RT-PCR

Total cellular RNA was extracted using ISOGEN II (Nippon Gene KK, Toyama, Japan). RNA samples were treated with 1 unit/μg DNase (RQ1; Promega, Madison, Wisconsin, USA) prior to RT-PCR. cDNA was synthesized from 2 μg RNA template according to the manufacturer's protocol (ReverTra-Ace-α RT–PCR kit; TOYOBO, Osaka, Japan). The expression level of each gene was normalized to that of *GAPDH*. The primer sequences are listed in Supplementary Table S1.

Transcriptome analysis

Transcriptome analysis was performed as previously described [18, 24]. Using the extracted total RNAs, microarray analysis was performed using an Agilent platform with 8 × 60 K design ID G4851B (Agilent Single Color. 39494, Agilent Technologies, Santa Clara, CA, USA). Subsequent gene annotation was conducted using GeneSpring software. Differentially expressed genes were defined by *p*-values of < 0.05 in the moderate *t*-tests after Benjamini-Hochberg corrections and fold change of > 2 or < 0.5. Gene set enrichment analysis (GSEA) was performed on the NB cells (SK-N-BE, SK-N-SH, NGP, and IMR32; Fig. 2). The a priori defined set of genes showed significant differences between the EPZ-6438 and 0.1% DMSO groups. KEGG Pathway analysis was performed on the IMR32 cells (Fig. 6c). Genes up- or down-regulated by more than + 2 or − 2 fold ($p < 0.05$) in EPZ-6438- and 5-aza-dC-treated IMR32 cells were analyzed using DAVID Bioinformatics Resources 6.8 (Laboratory of Human Retrovirology and Immunoinformatics Applied/Developmental Research Directorate Frederick National Laboratory for Cancer Research Frederick, MD, USA).

Overexpression experiments in NB cells

The gene cDNAs were cloned into the pcDNA3-neo vector (Thermo Fisher Scientific, USA). The plasmids were transfected into EPZ-6438-sensitive SK-N-BE cells in 6-cm-diameter culture dishes using the Fugene HD transfection reagent (Promega, Madison, WI, USA). After transfection, gene expression was confirmed by semi-quantitative RT-PCR. DNase treatment (Sigma-Aldrich) was performed to prevent plasmid contamination. Ten thousand cells were re-seeded into new 6-cm dishes and selected with 40 μg/mL of G418 (Sigma-Aldrich) for 3 weeks.

Chromatin immunoprecipitation (ChIP).

ChIP assays were performed as previously described [18]. Cross-linked chromatin prepared from the indicated cells was precipitated using normal rabbit IgG (Wako 148–09551), H3K27me3 rabbit pAb (Millipore).

Methylome analysis

DNA methylation analysis of the clinical data was performed using the Infinium HumanMethylation450 BeadChip Kit (Illumina, San Diego, CA, USA). The data

a

Sensitive cells (SK-N-BE, SH-N-SH) Up	NES	NOM p-val	FDR q-val
KONDO_EZH2_TARGETS	1.945395	0	0.062116
Resistant cells (NGP, IMR32) Up	**NES**	**NOM p-val**	**FDR q-val**
KONDO_EZH2_TARGETS	2.089804	0	0.0076

Sensitive cells change Down	NES	NOM p-val	FDR q-val
WHITFIELD_CELL_CYCLE_G1_S	-2.2753	0	0.001336
KEGG_CELL_CYCLE	-2.0455	0	0.006308
REACTOME_MITOTIC_PROMETAPHASE	-2.03103	0	0.006803
REACTOME_MITOTIC_M_M_G1_PHASES	-2.02904	0	0.006876
REACTOME_CELL_CYCLE_MITOTIC	-2.02681	0	0.006942
WHITFIELD_CELL_CYCLE_G2	-1.96355	0	0.010382
REACTOME_MITOTIC_G1_G1_S_PHASES	-1.91866	0	0.014698
REACTOME_MITOTIC_G2_G2_M_PHASES	-1.89142	0	0.01727
REACTOME_REGULATION_OF_MITOTIC_CELL_CYCLE	-1.76482	0	0.034718
Sensitive cells change Up	**NES**	**NOM p-val**	**FDR q-val**
GO_NEURAL_CREST_CELL_MIGRATION	1.820943	0	0.082807
GO_NEURAL_CREST_CELL_DIFFERENTIATION	1.725343	0	0.099985
GO_DENDRITE_DEVELOPMENT	1.583553	0.010204	0.117002

b

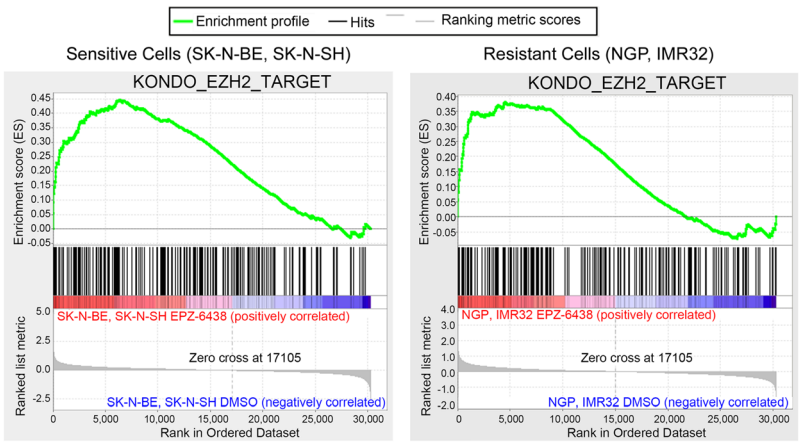

c

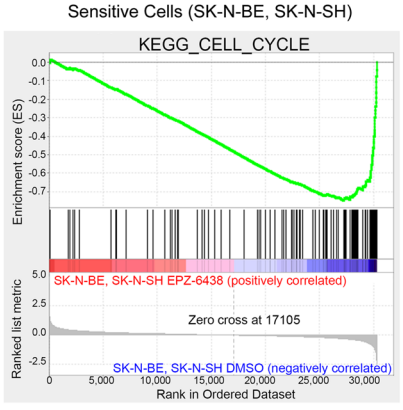

d

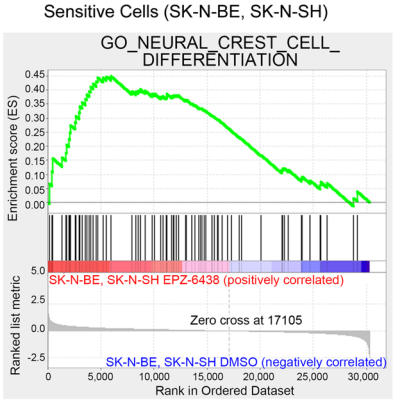

e Venn diagram FC > 2.0, p<0.05

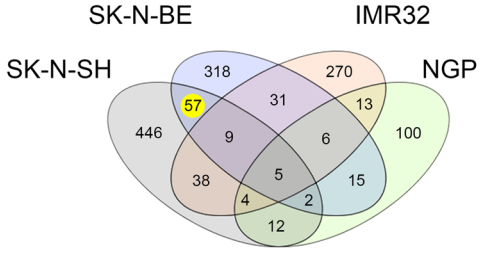

Fig. 2 (See legend on next page.)

(See figure on previous page.)

Fig. 2 Transcriptome analyses of EPZ-6438-treated neuroblastoma (NB) cells. NB cells were treated with 0.1% DMSO or 1 μM EPZ-6438. Total RNAs were extracted 3 days (SK-N-BE, SK-N-SH, NGP) or 4 days (IMR32) after the treatment. Data are representative of three independent experiments. We compared average gene expression levels between mock and EZH2 inhibitor (EZH2i)-treated cells and selected genes up- or down-regulated by more than 2-fold ($p < 0.05$) in EZH2i-treated cells **a** Results of a gene set enrichment analysis (GSEA) in sensitive (SK-N-BE and SK-N-SH) and resistant (NGP and IMR32) NB cells. FDR q-value < 0.25 and normalized p-value < 0.05 were used as criteria for significant enrichment **b** Heatmaps generated from microarray data showing genes included in KONDO_EZH2_TARGETS in sensitive and resistant cells **c**, **d** Heatmaps generated from microarray data showing genes included in KEGG_CELL_CYCLE (**c**) and GO_NEURAL_CREST_CELL_MIGRATION (**d**) in sensitive cells **e** A Venn diagram of differentially expressed genes more strongly upregulated by 1 μM EPZ-6438 in 4 NB cells than by 0.1% DMSO (Fold change > 2.0, $p < 0.05$). *P*-values were calculated using unpaired *t*-tests

were obtained from databases and patient samples we collected [1–3, 17, 25, 26]. DNA methylation analysis of IMR32 cells (Figs. 5 and 6) was performed using the Infinium MethylationEPIC Kit according to the manufacturer's protocol (Illumina, San Diego, CA, USA). Genomic DNA was extracted four days after inhibitor treatment. Data were adjusted using MACON at the Division of Epigenomics, National Cancer Center Research Institute (Tokyo, Japan) [27].

Combination index

Cells were seeded on 96-well plates (2000 per well) in 100 μl final volume. The medium was changed on days 0 and 2. The WST-8 assay was performed on days 3 or 4 and the effect was calculated (Effect = 1 – Sample/Control). Data were analyzed using CompuSyn software (ComboSyn, Inc., Paramus, NJ, USA).

Tumor formation in nude mice

All animal experiments were approved by the Saitama Cancer Center Animal Experiment Committee (Approval Number: 2024-5). Four-week-old female athymic BALB/c AJcl nu/nu mice (CLEA Japan, Shizuoka, Japan) were subcutaneously injected with 2×10^6 IMR32 cells in the presence of 50% Corning Matrigel, as described previously [18]. Each drug was dissolved in 100 μl of distilled water (Otsuka Pharmaceutical, Tokyo, Japan) containing 10% (2-hydroxypropyl)-β-cyclodextrin (Sigma-Aldrich, St. Louis, MO, USA). The drugs were administered intraperitoneally twice weekly (Control, 50 mg/kg EPZ-6438, and/or 0.25 mg/kg 5-aza-dC).

The tumor volumes were determined by measurements every day and the median tumor volume (V) was calculated as $V = (W^2 \times L)/2$ (V: Volume, W: Short diameter, L: Long diameter). The experimental endpoints were set at a tumor's longest diameter of 20 mm (L > 20 mm) or one month after injection. Animals reaching these endpoints were euthanized by cervical dislocation, and their tumors were surgically removed and collected. Data are shown as the mean ± SD of four xenografts twice weekly.

Pathological analysis

Pathological analysis was performed on formalin-fixed, paraffin-embedded tumor tissue sections. Ki-67 immunostaining was performed using a rabbit monoclonal anti-Ki-67 antibody (Dako, Denmark, 1:100 dilution) in a Bond-Max autostainer (Leica Biosystems, Buffalo Grove, IL, USA). The antigens were retrieved using a Bond Epitope Retrieval Solution 2 (Leica Biosystems) at 100 °C for 10 min.

Statistical analysis

For comparisons between two groups, we used either unpaired Student's *t*-tests. For multiple group comparisons, we applied Bonferroni correction, with a corrected p-value of < 0.05 considered statistically significant. All statistical analyses were performed using at least three independent biological replicates. All graphs present data as mean ± standard error of the mean (SEM). In gene expression analysis, we defined a significant difference as a fold change > ± 2 and a p-value < 0.05. For Gene Set Enrichment Analysis (GSEA), an FDR q-value < 0.25 and a normalized p-value < 0.05 were used as criteria for significant enrichment. Pathway analysis also considered a p-value < 0.05 as statistically significant for functional classification. For DNA methylation analysis, we obtained and normalized database and patient-derived data using the Illumina EPIC array. We identified significant methylation changes with a threshold of $p < 0.0001$.

Primer sequences for PCR experiments

These are indicated in Supplementary Table S1.

Results

The efficiency of EPZ-6438 against NB cell lines

Nine NB cell lines, SK-N-DZ, NB-69, SMS-SAN, NB-39-nu, IMR32, NGP, SH-SY5Y, SK-N-SH, and SK-N-BE, were used to examine EZH2i sensitivity using the WST-8 assay. The IC_{50} of DZNep, a nonselective EZH2i, was < 500 nM in the seven cell lines (Supplementary Fig. S1a). In addition, three cell lines, SH-SY5Y, SK-N-SH, and SK-N-BE, exhibited < 500 nM IC_{50} when treated with selective EZH2is, GSK126, or EPZ-6438 (Fig. 1a). Therefore, we selected SK-N-SH and SK-N-BE as sensitive NB cells and NGP and IMR32 as resistant NB cells against selective EZH2is. We examined the effects of different EPZ-6438 doses on sensitive and resistant NB cells using the WST-8 assay (Fig. 1b). We confirmed the EPZ-6438 sensitivity of the four NB cell lines using a colony formation assay (Fig. 1c). PI staining indicated that the number of cells in the G0/G1 phase increased and that in the S phase decreased in sensitive NB cells,

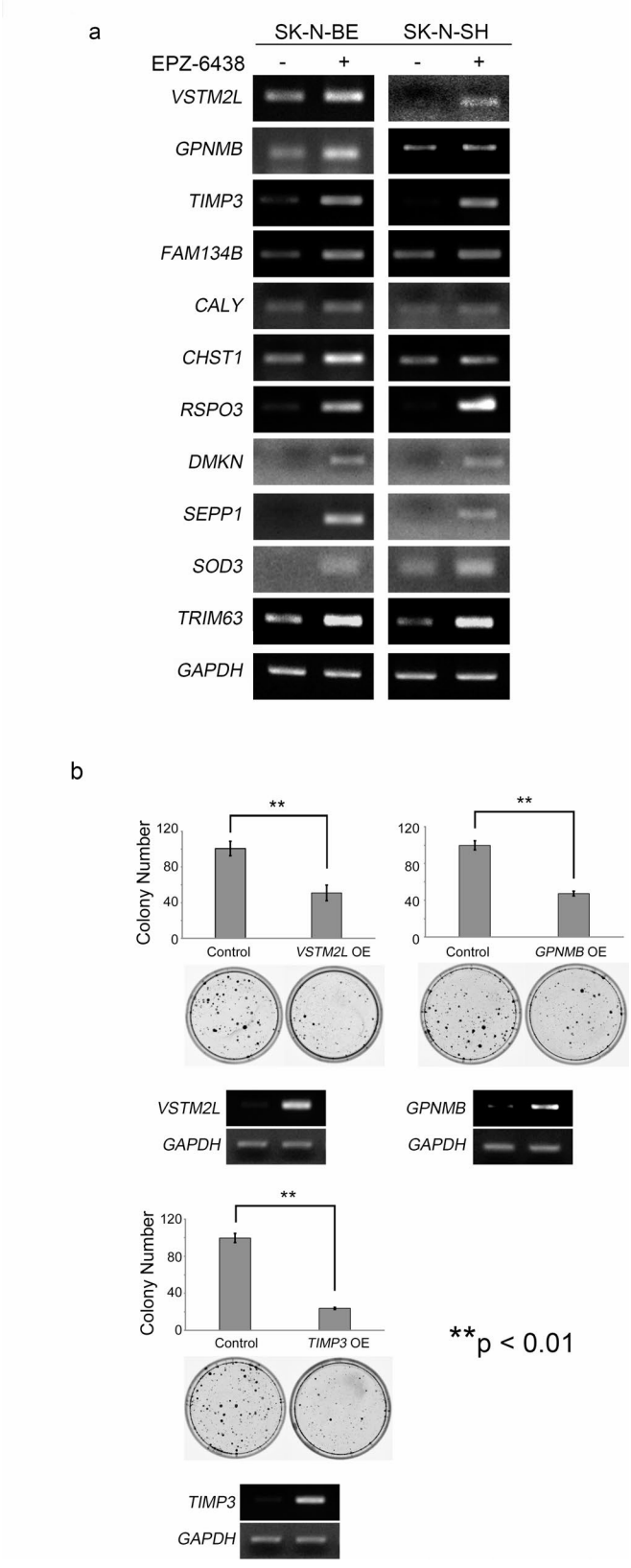

Fig. 3 (See legend on next page.)

(See figure on previous page.)

Fig. 3 Biological analysis of EZH2 inhibitor (EZH2i)-induced genes in EZH2i-sensitive neuroblastoma (NB) cells **a** Semi-quantitative RT-PCR analyses of EZH2i-sensitive SK-N-BE and SK-N-SH cells treated with DMSO (–) or 1 μM EPZ −6438 (+) for 3 days. Semi-quantitative RT-PCR was performed to analyze EZH2i-induced genes in EZH2i-sensitive cells selected based on the microarray results **b** Colony formation assay of VSTM2L-, GPNMB- and TIMP3- expressing NB cells. EZH2i-sensitive SK-N-BE cells were seeded in 6-cm dishes (5×10^5 cells per dish) after transfection with pcDNA3 (empty, VSTM2L, GPNMB, TIMP3, or TRIM63). The results obtained are presented as the mean ± SD of at least three independent experiments. The lower panels show semi-quantitative RT-PCR analyses of SK-N-BE cells after transfection. The results obtained are presented as the mean ± SD of at least three independent experiments. *P*-values were calculated using Student's *t*-tests

but not resistant NB cells (Fig. 1d). EZH2 is a histone methyltransferase that catalyzes histone H3 lysine 27 (H3K27) methylation. Therefore, we investigated the effects of EPZ-6438 on H3K27me3. Briefly, 1 μM EPZ-6438 almost completely inhibited H3K27 methylation within 4 days in both EZH2i-sensitive and -resistant cell lines (Fig. 1e). Furthermore, 1 μM EPZ-6438 effectively inhibited H3K27me3, H3K27me2, and H3K27me1 in a dose-dependent manner (Fig. 1f); however, no significant differences were observed between sensitive and resistant NB cells. EPZ-6438 reduced *EZH2* mRNA levels in sensitive NB cells, but not resistant cells (Supplementary Fig. S1b, c, and d). In addition, EZH2 protein levels decreased only in sensitive NB cells.

EPZ-6438 sensitivity to transcriptome

To elucidate the effects of EPZ-6438 on genome-wide gene expression profiles, we performed a transcriptome analysis using expression microarrays. GSEA showed that KONDO_EZH2_TARGETS (M5301) was significantly upregulated in both sensitive and resistant NB cells, suggesting that the EPZ-6438 treatment effectively derepressed EZH2 targets in NB cells (Fig. 2a and b) [28]. Several cell cycle progression-related pathways, such as WHITFIELD_CELL_CYCLE_G1_S (M2074, NES − 2.2753); KEGG_CELL_CYCLE (M7963, NES − 2.0455), were significantly downregulated in sensitive NB cells (Fig. 2c), but not resistant NB cells (data not shown). Neural crest migration/differentiation-related pathways were upregulated in sensitive NB cells (Fig. 2d), which was consistent with the results of our previous EZH2 knockdown experiments [18]. Since EZH2 functions as a H3K27me3 modification-mediated transcription suppressor, EZH2 inhibition may upregulate the expression of its target genes. Fifty-seven upregulated genes in sensitive NB cells [fold change (FC) > 2, $p < 0.05$] (Supplementary Table S2), but not resistant NB cells, were defined (moderate *t*-test $p < 0.05$, FC > 2.0; Fig. 2e).

We then identified 25 genes from the 57 genes upregulated by EZH2i in the sensitive cells, which were associated with good prognosis in NB patients according to the R2 database (Genomics Analysis and Visualization Platform, https://hgserver1.amc.nl/). Based on these results, we further examined the expression of 11 genes identified by ChIP-seq as H3K27me3-regulated in the EZH2i-sensitive cell line SK-N-BE (BE2C), and possessing CpG islands near their transcription start sites (TSS), using semi-quantitative RT-PCR. (Fig. 3a, Supplementary Table S3). We then identified three potential tumor suppressor genes strongly associated with a favorable prognosis in patients with NB (Supplementary Fig. S2a-S2d). Among these genes, we focused on *VSTM2L*, *GPNMB*, and *TIMP3*, further confirming their functions as tumor suppressors using a colony formation assay. While overexpression of *TRIM63* inhibited colony formation, similar to other genes. However transcription of *TRIM63* was not only regulated by EZH2-dependent H3K27me3 (Supplementary Figure S4). The overexpression of these genes effectively suppressed colony formation in EZH2i-sensitive SK-N-BE cells (Fig. 3b).

Synergistic NB cell growth suppression by EZH2i and DNMTi combination

Although single DNMTi treatments suppressed proliferation, additional EZH2i treatments suppressed proliferation significantly more than the single treatments (Fig. 4a). These inhibitors synergistically suppressed IMR32 proliferation because the combination index (CI) was < 1.0; these synergistic effects were also observed in the three other resistant NB cell lines (Fig. 4b; Supplementary Fig. S5). We also examined the in vivo effects of EZH2i and DNMTi on resistant IMR32-derived tumors treated with 50 mg/kg EPZ-6438 or 0.25 mg/kg 5-aza-dC. Combined treatment with EZH2i and DNMTi in xenograft experiments also significantly suppressed tumor growth (Fig. 4c), and Ki-67-positive cells decreased in combination-treated NB tumors (Fig. 4d).

DNA methylation of EZH2i sensitivity-related genes

Epigenetically regulated genes can be controlled not only by histone modifications but also by DNA methylation. Particularly, genes involved in cell differentiation and lineage commitment are often silenced in differentiated cells within tissues by more robust DNA methylation, rather than by reversible histone modifications. Then, we hypothesized that DNA methylation, another epigenetic regulatory mechanism, is responsible for maintaining EZH2i sensitivity. Previous studies have shown that DNA methylation plays a role in determining the characteristics of NB and influences patient prognosis [1–3, 25]. Therefore, we examined genomic DNA methylation status using Infinium HumanMethylation450 BeadChip Kit-produced data. We confirmed the presence or absence of CpG islands in these regions (Fig. 5a) and detected the

Figure 4

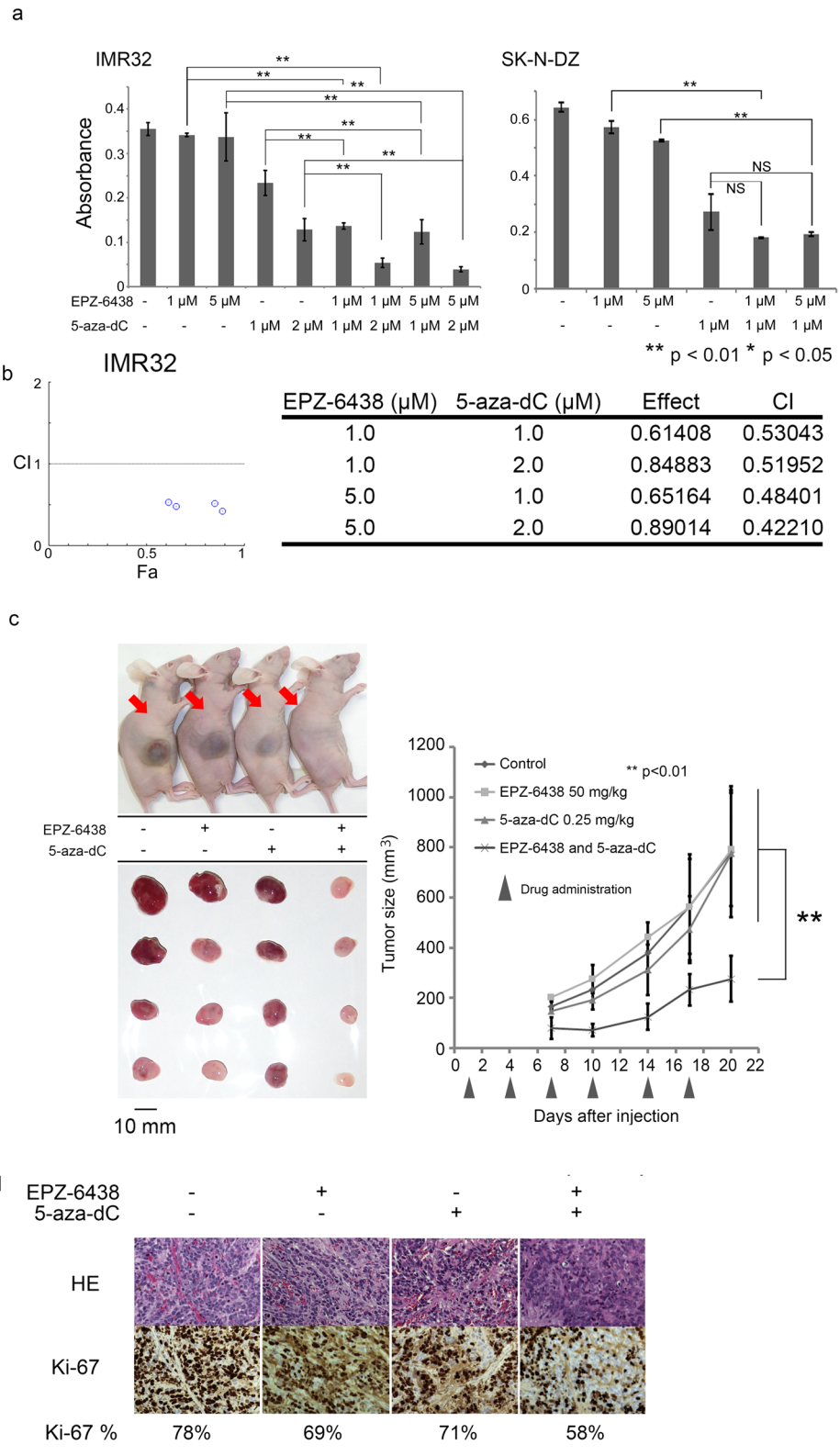

Fig. 4 (See legend on next page.)

(See figure on previous page.)

Fig. 4 Synergistic effects of EPZ-6438 and 5-aza-dC on EPZ-6438-resistant neuroblastoma (NB) cells **a** Proliferation assay was performed using the WST assay. Cells were seeded in 96-well plates (2000 per well). Results were obtained four days after treatment and indicated as the mean ± SD of at least three independent experiments. *P*-values were calculated using Student's *t*-tests with Bonferroni correction **b** The combination index (CI) showing the synergistic effects of EPZ-6438 and 5-aza-dC on IMR32 cells. CI was calculated from WST assay results (Effect = 1 − Sample/Control), and analyzed with CompuSyn software (CompuSyn.) **c** Xenograft formation in BALB/c AJcl nu/nu mice following the injection of IMR32 under intraperitoneal drug administration (Control, 50 mg/kg EPZ-6438, and/or 0.25 mg/kg 5-aza-dC) twice per week. The tumors were measured twice a week after injection. Data were presented as the mean ± SD of four xenografts. *P*-values were calculated using Student's *t*-tests with Bonferroni correction **d** Immunohistochemical analysis by Hematoxylin-Eosin staining and Ki-67

DNA methylation of these CpG islands in 8 out of 25 gene regions. Among the eight genes, *VSTM2L*, *GPNMB*, and *TIMP3* promoter CpG islands were methylated in some patients with NB (Supplementary Fig. S3), and the methylation status was inversely related to gene expression (Fig. 5b). Furthermore, *VSTM2L* and *GPNMB* CpG high beta values were related to advanced stages of NB and *MYCN* amplification (Fig. 5b and c). The beta values of the CpG probe in the *TIMP3* region (cg05470389 and cg20500237) were high in *MYCN* non-amplified NB (Fig. 5d). Most patients with high beta values at *TIMP3* regions (≥ 0.5) had a poor prognosis (death or relapse/progression: 34/57 = 0.60), advanced clinical stages (INSS3 or 4:45/57 = 0.79), and onsets at older ages (onset ages > 18 months: 47/57 = 0.82) (Supplementary Table S4). DNA hypomethylation of CpG islands is correlated with high expression of these genes (Fig. 5e and g).

Transcriptome analysis by EZH2i and DNMTi combination in NBs

Since DNA methylation represents another gene expression repression mechanism to EZH2, we investigated the anti-tumor effects of the combined treatment with EZH2i (EPZ-6438) and DNMTi (5-aza-dC) in EZH2i-resistant IMR32 cells. Mock-, 1 μM EPZ-6438-, 1 μM 5-aza-dC-, and combination-treated IMR32 cells were subjected to expression and DNA methylation microarray analyses (Fig. 6).

We first examined the expression of 25 EZH2i sensitivity-related genes in IMR32 cells treated with a combination of EZH2i and DNMTi (Fig. 6a, Supplementary Fig. S6a). The combination treatment significantly upregulated *VSTM2L*, *GPNMB*, and *TIMP3* which was accompanied with promoter CpG region demethylation. H3K27me3 levels upstream of the TSS for these genes decreased in both EZH2i sensitive and resistant cells upon EZH2i treatment. This reduction in H3K27me3 was more pronounced in EZH2i sensitive cells, suggesting that in resistant cells, gene repression by DNA methylation and H3K27me3 near the TSS might be mutually exclusive (Supplementary Fig. S6b-g). Some EZHi sensitivity-related expressed genes, such as *AATK*, *RSPO4*, and *TRIM63*, were downregulated in EZH2i- and DNMTi-treated EZH2i-resistant IMR32 cells. These findings suggest that only epigenetic unlocking is insufficient to commit all cells to an adrenergic neuronal lineage.

We characterized 1469 upregulated genes (FC > 2.0, $p < 0.05$) in the combination treatment (Supplementary Table S5) using pathway analysis (DAVID Bioinformatics Resources 6.8). The pathway analysis against the KEGG Pathway showed several neuronal differentiation-associated pathways, such as "Serotogenic synapse (hsa04726)" and "Axon guidance (hsa04360)" were enriched (Fig. 6b, Supplementary Fig. S7a and S7b). Furthermore, tumor suppression-related pathways, including "TNF-signaling pathway (hsa04668)," were significantly enriched (Fig. 6b). In addition, neuronal functions-associated pathways such as "Amphetamine addiction," "Glutamatergic synapse," and "Nicotine addiction" indicated the clear de-repression of the genes of these pathways and some promoter CpG island demethylation by DNMTi treatment, suggesting a role for demethylation effects on promoter regions in de-repression (Fig. 6b).

DNMTi-induced MYCN downregulation suppresses cell cycle in NB cells

To elucidate the combined effects on the cell cycle, we performed transcriptome analysis. Pathway analysis of downregulated genes in IMR32 cells showed that the "DNA replication" and "cell cycle" pathways were significantly suppressed after combined treatment with EZH2i and DNMTi (Fig. 6c and d). The genes involved in these pathways were downregulated by DNMTi treatment, and their expression was further suppressed by combination treatment with EZH2i (Fig. 6d, Supplementary Fig. S7c). *POLE*, *MCM6*, *PCNA*, *RFC4*, *SKP2*, *CDC20*, *CDK2*, and *PRKDC*, which are well-established MYC target genes, were identified in multiple gene sets, including "HALLMARK_MYC_TARGETS_V1" [29]. We thus assessed MYCN expression in the EZH2i- and DNMTi-treated NB cells. MYCN was clearly downregulated at the protein level in DNMTi-treated IMR32, SK-N-DZ and NGP cells (Fig. 6e) The mRNA levels of *MYCN* did not correlate with the protein levels in IMR32 and SK-N-DZ. (Supplementary Fig. S7d). Furthermore, a similar decrease was observed in NGP cells with MYCN amplification. In NB-69 cells without MYCN amplification, a decrease in c-MYC, rather than MYCN, was observed. This decrease of c-MYC was also observed in 293 T cells, a human cell line that highly expresses c-MYC (Fig. 5f). *c-MYC* transcription was reduced by treatment with EZH2i and DNMTi both in NB-69 and 293 T cells (Supplementary

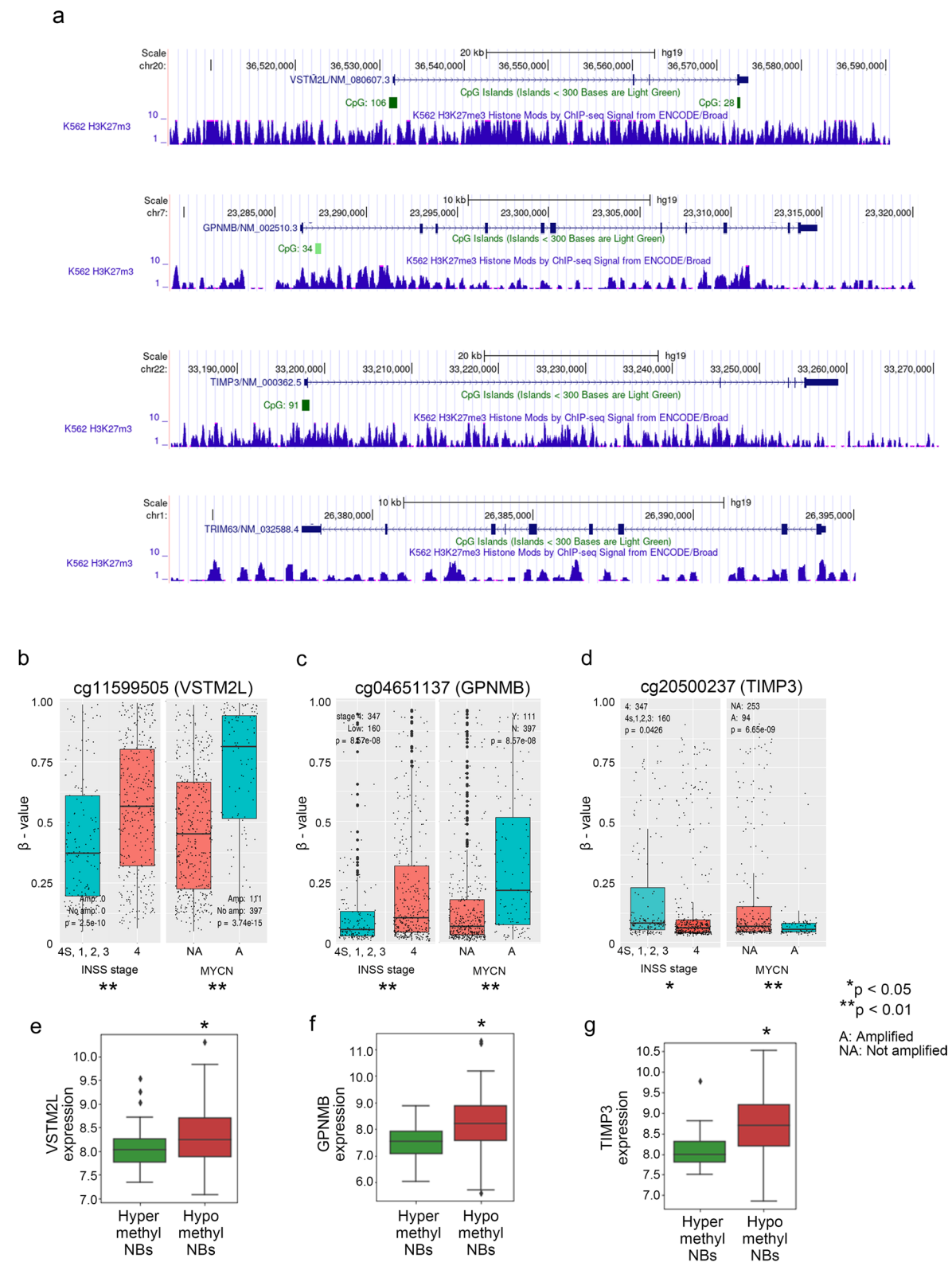

Fig. 5 (See legend on next page.)

(See figure on previous page.)

Fig. 5 Epigenetic analysis of EZH2i-induced genes in neuroblastoma (NB) **a** Track views of several sensitive cell-specific genes identified in Fig. 2. Visualization was generated using the UCSC Genome Browser (https://genome.ucsc.edu/cgi-bin/hgTracks), based on the Human (GRCh37/hg19) reference genome **b** Comparison of DNA methylation levels of *VSTM2L* (**b**), *GPNMB* (**c**), and *TIMP3* (**d**) promoters in the (1) INSS1-3, 4 S/INSS4; (2) *MYCN*-amplified (MA)/not-amplified (MNA) samples. Data are from Ref. 2. The expression of *VSTM2L* (**e**), *GPNMB* (**f**), and *TIMP3* (**g**). Data are from Ref. 2 and are presented as bar graphs according to the CGI status (hypomethylated: beta value < 0.5; hypermethylated: beta value ≥ 0.5). *: $p < 0.05$. *P*-values were calculated using unpaired *t*-tests

Fig. S7e). These results suggested that the mechanisms of c-MYC and MYCN reduction by DNMTi treatment were quite different, with *c-MYC* being initially reduced at the mRNA level. These findings suggest that DNMTi may affect some factors involved in MYCN protein stabilization, leading to MYC destabilization (Supplementary Fig. S5). These results suggest that EZH2i mainly derepresses cellular differentiation pathways, and DNMTi suppresses MYC-related pathways. Consequently, combined treatment with EZH2i and DNMTi is anticipated to enhance the ability to inhibit NB cell growth through multiple mechanisms.

Discussion

EZH2, a component of PRC2, is overexpressed in various types of cancer. In NB, *EZH2* mRNA overexpression correlate with poor prognosis [22]. However, targeted therapies against EZH2 in malignant NB have been limited, and mutations in *ARID1A*, a gene relevant for selecting EZH2is, are rare [23, 30]. Moreover, in NB, 7q36, where EZH2 is located, is frequently observed, and quantitative abnormalities in EZH2 are involved in H3K27me3 methylation-independent cancer malignancy [16]. In this study, we identified multiple genes derepressed in EZH2i-sensitive NB cells in an EZH2i-dependent manner. The combination of EZH2i and DNMTi was effective against EZH2i-resistant cells. When EZH2is were administered to multiple NB cell lines, effective anti-tumor concentrations varied among the cell lines. Consequently, numerous studies have explored the novel genomic mutations associated with responsiveness [17, 20, 21]. Despite extensive research, a robust correlation between specific genetic mutations and the response to EZH2i in NB remains elusive.

Based on our findings, we hypothesized that distinct gene expression profiles underlie the differential sensitivity of NB cells to EZH2i. Microarray analysis revealed several differentially expressed genes in EZH2i-sensitive and -resistant cells. While most NB cells exhibit modest morphological changes upon EZH2 inhibition, accompanied by the induction of genes associated with neuronal differentiation, EZH2i-sensitive cells demonstrate a marked induction of tissue-specific gene expression programs typically associated with non-neuronal tissues. *VSTM2L* encodes a secreted protein with a transmembrane domain. It is downregulated in nerve and adrenal gland tissues, but upregulated in brain tissue [31]. *GPNMB* also encodes a membrane glycoprotein that is expressed in mature microglia and liver cells [32, 33]. *TIMP3* codes an extracellular protein that suppresses the metalloprotease activity of MMPs [34]. *TRIM63* encodes a transcription factor involved in muscle development [35]. While these genes may not directly regulate cell cycle suppression, four seem to influence nerve, liver, muscle, and epithelial tissue differentiation. Typically, epigenetically regulated genes control cell fate to suppress inappropriate lineages, such as adrenal gland or sympathoadrenal tissue gene expression. EPZ-6438 induced aberrant differentiation in EZH2i-sensitive cells, but not EZH2i-resistant cells. Our previous study demonstrated that EZH2 depletion via short hairpin RNA in EZH2i-resistant cells resulted in morphological changes consistent with neuronal differentiation. Additionally, gene expression profiles indicative of differentiation into various tissues, including pancreatic tissues, have been reported [18]. On the other hand, since NB cells treated with EPZ-6438 showed little morphological change despite reduced H3K27 methylation, this suggested a non-canonical effect of EZH2 in the knockdown experiment. Moreover, many candidate tumor suppressor genes found in this study, which are associated with a favorable prognosis in NB, harbor CpG islands near their transcription start sites, and poor prognosis correlates with hypermethylation. The *NTRK1* gene was subject to robust transcriptional repression via H3K27 methylation and DNA methylation at two critical promoter regions [18]. These results indicate that the genes not associated with tissue-specific differentiation or tumor suppression were subject to coordinated repression by EZH2-dependent H3K27me3 and DNA methylation in NBs.

EZH2- and DNMT-mediated epigenetic silencing often target genes involved in cell differentiation. The combined inhibition of EZH2 and DNMTs or HDACi may derepress these genes and tumor suppressors. Previous studies have reported using 5-aza-dC, HDAC and DOT1L inhibitors in combination with EZH2 or PRC2 inhibitors to enhance their therapeutic effects [17, 24, 36–40], as these agents synergize in reversing gene silencing. Combination of EZH2is and 5-aza-dC potentiated differentiation and suppressed cell cycle progression. In malignant NB, *MYCN* amplification is a key tumorigenesis driver. In *MYCN* non-amplified cells such as NB-69, elevated *c-MYC* expression has been implicated in tumorigenesis. While previous studies have shown that 5-aza-dC can

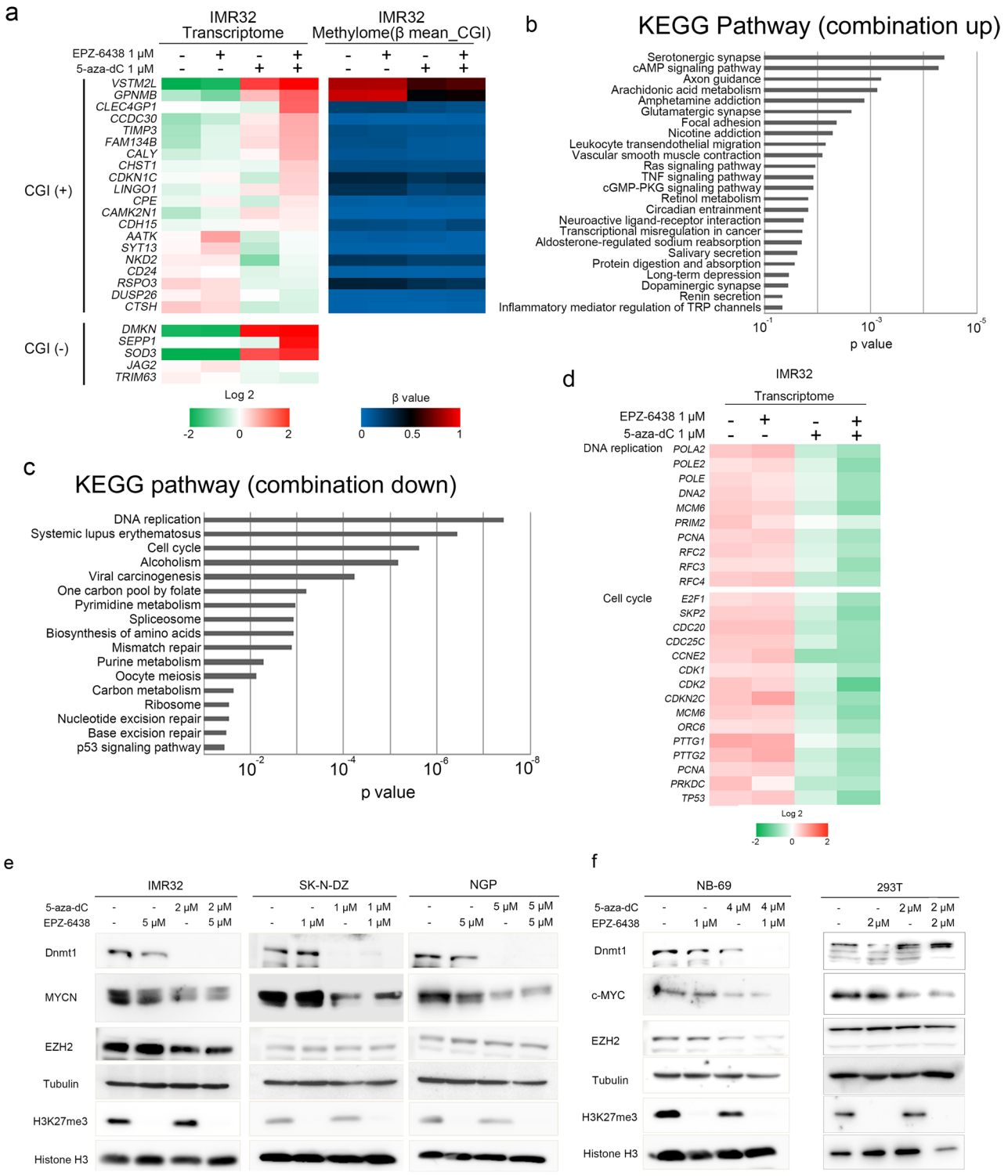

Fig. 6 (See legend on next page.)

(See figure on previous page.)

Fig. 6 Transcriptome and methylome analyses of EPZ-6438- and 5-aza-dC-combination-treated IMR32 cells **a** Heatmaps generated from microarray or methylome data showing expression profiles of genes associated with EZH2i sensitivity in IMR32 cells treated with EZH2i and/or 5-aza-dC. EZH2i-induced genes in EZH2i-sensitive cells were selected based on microarray results **b** Results of KEGG Pathway analysis (DAVID Bioinformatics Resources 6.8) for genes upregulated more than + 2 fold ($p < 0.05$) in IMR32 cells treated with EPZ-6438 and 5-aza-dC. *P*-values were calculated using unpaired *t*-tests **c** Results of pathway analysis using the KEGG Pathway (DAVID Bioinformatics Resources 6.8) for genes downregulated by more than − 2 fold ($p < 0.05$) in EPZ-6438- and 5-aza-dC-treated IMR32 cells. *P*-values were calculated using unpaired *t*-tests **d** Heatmaps generated from microarray data showing expression profiles of genes associated with cell proliferation or cell cycle pathways in EZH2i- and/or 5-aza-dC-treated IMR32 cells, where these pathways correspond to the 'DNA replication' and 'Cell cycle' gene sets in Fig. 5c **e** MYCN downregulation by combination treatment with EPZ-6438 and/or 5-aza-dC. Western blot analysis was performed on NB cells after four days of treatment with the indicated drug concentrations **f** c-MYCN downregulation by combination treatment with EPZ-6438 and/or 5-aza-dC in NB-69 and 293T cells

decrease *c-MYC* gene expression at the transcriptional level [41, 42]. On the other hand, *MYCN* transcription is not thought to be entirely the same as *c-MYC*, and a consistent effect was not obtained with DNMTi in NB cells. Our data suggest that DNMTi may also affect the stability of the MYC family proteins, MYCN and c-MYC. The instability of MYC protein levels is thought to be due to MYCN or c-MYC being included in some molecular complex targeted by DNMTi, but this has not yet been fully elucidated. Since MYCN can upregulate EZH2 and other PRC2 components [14], prolonged treatment with DNMTi may reduce MYCN levels, subsequently decreasing PRC2 levels and further inhibiting cell cycle progression. However, multiple observations of a tendency for *MYCN* mRNA to decrease upon combined treatment with an EZH2i and DNMTi suggest that EZH2 inhibition may be involved in regulating factors suppressing the transcriptional activation of the *MYC* gene.

This study demonstrated that the combination of EZH2is and DNMTi exhibits enhanced efficacy both in vitro and in vivo. While EZH2is have shown promise in cancers harboring activating mutations in EZH2, such as DLBCL, elevated PRC2 activity is a common feature in many cancers [43–45]. However, the emergence of EZH2 variants resistant to inhibitors like GSK343 or DS-3201 (Valemetostat) has limited the clinical utility of EZH2is [46, 47]. On the contrary, in some cancers, mutations in EZH2 or DNMT3 result in the loss of H3K27 methylation and DNA methylation across a broad spectrum of genes, including those involved in differentiation and tumor suppression [48–51]. In these cells, the loss of these repressive epigenetic marks is likely compensated for by other gene silencing mechanisms. Therefore, our approach of targeting multiple gene repression mechanisms offers a novel strategy for inducing differentiation and inhibiting the proliferation of various cancers.

Our results suggest that the combination of clinically approved PRC inhibitors such as EPZ-6438 and DS-3201 with demethylating agents such as 5-aza-dC may offer an effective therapeutic strategy, particularly for *MYCN*-amplified NB. Furthermore, we revealed a novel therapeutic mechanism where the combination of EZH2i and DNMTi not only potently promotes cell differentiation, but also induces MYC protein reduction.

Conclusions

Gene sets mainly related to cell differentiations, which are involved in the suppression of NB growth, are epigenetically repressed through multiple regulatory pathways mediated by EZH2 and DNMTs. And these mechanisms vary depending on the cell type. The combination of EZH2i and DNMTi strongly suppressed the growth of NB cells, and DNMTi was found to reduce MYCN and c-MYC at protein levels.

Abbreviations

EZH2	Enhancer of Zeste Homolog 2
NB	neuroblastoma
EZH2i	EZH2 inhibitor
DNMT1	DNA Methyltransferase 1
DNMTi	DNA methyltransferase inhibitor
H3K27	Histone H3 lysin 27
H3K27me3	Trimethyl-Histone H3 (Lys27)
GSEA	Gene Set Enrichment Analysis

Supplementary Information

The online version contains supplementary material available at https://doi.org/10.1186/s12885-025-14882-7.

Supplementary Material 1: Supplementary Figure S1 EZH2 inhibitor sensitivity differences in neuroblastoma (NB) cell lines. a IC_{50} values for each cell line treated with the nonselective EZH2 inhibitor, DZNep. NB cell proliferation was assessed using the WST assay. b, c, d EZH2 mRNA expression following dose- and time-dependent EPZ-6438 treatment. Data were obtained by semi-quantitative PCR (b) and qPCR experiments as described in the "Methods." (c) Time-dependent and (d) dose-dependent results were normalized to ACTIN expression.

Supplementary Material 2: Supplementary Figure S2. Kaplan–Meier survival analysis of patients with neuroblastoma based on higher or lower expression levels of *VSTM2L* (a), *GPNMB* (b), *TIMP3* (c), and *TRIM63* (d) (event-free survival analysis) presented using a microarray analysis of two individual cohorts, SEQC and Kocak in the R2 website (https://hgserver1.amc.nl/cgi-bin/r2/main.cgi). Gene expression levels were separated into a high or low group based on average expression levels. A statistical analysis was performed using the Log-rank test. Corresponding Bonferroni *p* values (bonf p) are indicated.

Supplementary Material 3: Supplementary Figure S3. A heatmap analysis of DNA methylation in clinical NB samples derived from Japan (JPN, n=145, Ohira et al., manuscript in preparation) [1], [2], [3], [25]. Blue, red, and gray colors denote low, high, and intermediate DNA methylation levels, respectively. Information on the probes is described in the "Methods." The heat map shows CGI (TSS ± 2000 bp) methylation in genes (*VSTM2L*, *TIMP3*, and *GPNMB*). Probe numbers are indicated below the heat map.

Supplementary Material 4: Supplementary Figure S4. Colony formation assay of TRIM63-expressing NB cells. The results obtained are presented as the mean ± SD of at least three independent experiments. P-values were calculated using Student's *t*-tests.

Supplementary Material 5: Supplementary Figure S5. Synergistic effects of EPZ-6438 and 5-aza-dC on EZH2i-resistant cells. a–c Combination index (CI) shows the synergistic effects of EPZ-6438 and 5-aza-dC on SK-N-DZ, NB-69, and NGP cells. CI was calculated from WST assay results (Effect = 1 − Sample/Control) and analyzed with CompuSyn software (CompuSyn, Inc., Paramus, NJ, USA).

Supplementary Material 6: Supplementary Figure S6. a semi-quantitative RT-PCR analyses of treated IMR32 cells. RNA extraction and semi-quantitative RT-PCR were performed as described in the "Methods.". b-d, qChIP at TSS-proximal regions of representative genes in EZH2i-sensitive SK-N-BE cells. e-g, qChIP at TSS-proximal regions of representative genes in EZH2i-resistant IMR32 cells.

Supplementary Material 7: Supplementary Figure S7. a, b Heatmaps generated from microarray data indicating genes included in KEGG_SEROTOGENIC_SYNAPSE (c-1) and KEGG_AXON_GUIDANCE (c-2). CGI methylation was examined using an Infinium HumanMethylation450 BeadChip Kit (Illumina, San Diego, CA, USA). c Semi-quantitative RT-PCR analyses of cell cycle-related genes in EZHi- and/or DNMTi-treated IMR32 cells. d The qPCR analysis of MYCN in EZHi- and/or DNMTi-treated IMR32 and SK-N-DZ cells. e The qPCR analysis of c-MYCN in NB-69 and 293cells.

Supplementary Material 8: Supplementary Table S1. List of primers used in this study. Procedures. Primers used for qRT-PCR. (??).

Supplementary Material 9: Supplementary Table S2. Prognostic analysis of 57 genes from Fig. 2e using the R2 database.

Supplementary Material 10: Supplementary Table S2. Information on 57 patients with high (>0.5) beta values at cg20500237. Important clinical information and beta values for cg20500237 are presented.

Supplementary Material 11: Supplementary Table S3. H3K27me3 peak definitions were determined using ChIP-Seq data from databases. Fold-changes in gene expression were determined using the microarray data shown in Fig. 2. CpG islands (CGI) was identified as described in the "Methods" section. NB tumor CGI methylation was assessed using [1], [2], [3], [18], [25], [26].

Supplementary Material 12: Supplementary Table S4. Beta-value of cg20500237 in neuroblastoma (NB) patients from tumor databases.

Supplementary Material 13: Supplementary Table S5. EPZ-6438/5-aza-dC upregulated 1469 genes in IMR32 cells (Fig. 5).

Acknowledgements
We thank Ms. K Tachikawa and Ms. N Kawanabe for their technical assistance. The authors would like to thank Editage (http://www.editage.jp) for their assistance in the English language editing process.

Authors' contributions
Y.E. and H.T. wrote the main manuscript text and E.F. prepared Figs. 1, 2, 3, 4, 5 and 6 and all supplementary materials.R.P.S. curated data and made programs and prepared Figs. 2, 4 and 5, supplementary S3 and S4. M.O. edited the main manuscript text and curated data in Figs. 4 and 5.K.M., J.A., S.S., Y.S., R.O. and M.H. analyzed data in Figs. 1, 5 and 6, supplementary S4 and S5.N.H. and T.U. supported to analysis of figures 4 and supplementary S3.At. N. visualized and analyzed figure 6. T.K. wrote the main manuscript text and administrated this project.Ak.N., M.N. and T.K. supervised this project.

Funding
This work was supported by JSPS KAKENHI, Grants-in-Aid for Scientific Research, Japan Society for the Promotion of Science. Grant Numbers JP20K08174, JP24K10101, JP20K08269, JP19H03625.

Data availability
The datasets supporting the conclusions of this study are available in the NCBI GEO database. Transcriptome analysis of Cell line DMSO [GSE143714]/EPZ-6438 [GSE143713]. Transcriptome analysis of IMR32 5-aza-dC [GSE162058]/EPZ-6438 [GSE143712]. Methylome analysis of IMR32 5-aza-dC/EPZ-6438 [GSE162059].

Declarations

Ethics approval and consent to participate
All animal experiments were approved by the Saitama Cancer Center Animal Experiment Committee (Approval Number: 2024-5).

Consent for publication
Not applicable.

Competing interests
The authors declare no competing interests.

Author details
[1]Research Institute for Clinical Oncology, Saitama Cancer Center, 818 Komuro, Ina 362-0806, Saitama, Japan
[2]Department of Pediatric Surgery, Tohoku University Graduate School of Medicine, 1- 1, Seiryo-machi, Aoba-ku, Sendai 980-8574, Miyagi, Japan
[3]Laboratory of Tumor Molecular Biology, Department of Graduate School of Science and Engineering, Saitama University, 255 Shimo-okubo, Sakura-ku, Saitama 338-8570 Saitama, Japan
[4]Department of Pediatric Surgery, Chiba University Graduate School of Medicine, 1- 8-1 Inohana, Chuo-ku, Chiba 260-0856 Chiba-shi, Chiba, Japan
[5]Division of Epigenomics, National Cancer Center Research Institute, 5-1-1, Tsukiji, Chuo-ku, Tokyo 104-0045 Tokyo, Japan
[6]Laboratory of Integrative Metabolic Regulation, Institute for Molecular and Cellular Regulation, Gunma University, 3-39-15 Showamachi, Maebashi-shi, Gunma 371-0034, Japan
[7]Department of Clinical Research, Saitama Children's Medical Center, 1-2 Shintoshin, Chuo-ku, Saitama 330-8777 Saitama, Japan
[8]Department of Epigenomics, Institute for Advanced Life Sciences, Hoshi University, 2-4-41 Ebara, Shinagawa-ku, Tokyo 142-8501 Tokyo, Japan
[9]Saga Heavy Ion Medical Accelerator in Tosu, 3049 Koga-cho, Tosu 841-007, Saga, Japan

Received: 23 April 2025 / Accepted: 18 August 2025
Published online: 12 November 2025

References

1. Pugh TJ, Morozova O, Attiyeh EF, Asgharzadeh S, Wei JS, Auclair D, et al. Maris JM the genetic landscape of high-risk neuroblastoma. Nat Genet. 2013;45:279–84. https://doi.org/10.1038/ng.2529. Epub 2013 Jan 20. PMID: 23334666.
2. Schramm A, Köster J, Assenov Y, Althoff K, Peifer M, Mahlow E, et al. Schulte JH mutational dynamics between primary and relapse neuroblastomas. Nat Genet. 2015;47:872–7. https://doi.org/10.1038/ng.3349. Epub 2015 Jun 29. PMID: 26121086.
3. Gómez S, Castellano G, Mayol G, Suñol M, Queiros A, Bibikova M, et al. Lavarino C DNA methylation fingerprint of neuroblastoma reveals new biological and clinical insights. Epigenomics. 2015;7(7):1137–53. https://doi.org/10.2217/epi.15.49. Epub 2015 Jun 12. PMID: 26067621.
4. Valentijn LJ, Koster J, Zwijnenburg DA, Hasselt NE, van Sluis P, Volckmann R, et al. TERT rearrangements are frequent in neuroblastoma and identify aggressive tumors. Nat Genet. 2015;47:1411–4. https://doi.org/10.1038/ng.3438.
5. Peifer M, Hertwig F, Roels F, Dreidax D, Gartlgruber M, Menon R, et al. Fischer M telomerase activation by genomic rearrangements in high-risk neuroblastoma. Nature. 2015;526:700–4. PMID: 26466568.
6. Molenaar JJ, Koster J, Zwijnenburg DA, van Sluis P, Valentijn LJ, van der Ploeg I, et al. Versteeg R sequencing of neuroblastoma identifies chromothripsis and defects in neuritogenesis genes. Nature. 2012;483:589–93. https://doi.org/10.1038/nature14980. Epub 2015 Oct 14. PMID: 22367537.
7. Abe M, Ohira M, Kaneda A, Yagi Y, Yamamoto S, Kitano Y, et al. CpG Island methylator phenotype is a strong determinant of poor prognosis in neuroblastomas. Cancer Res. 2005;65(3):828–34. PMID: 15705880.
8. Ridinger J, Koeneke E, Kolbinger FR, Koerholz K, Mahboobi S, Hellweg L, et al. Dual role of HDAC10 in lysosomal exocytosis and DNA repair promotes neuroblastoma chemoresistance. Sci Rep. 2018;8:10039. https://doi.org/10.1038/s41598-018-28265-5. PMID: 29968769.

9. Casciano I, Banelli B, Croce M, De Ambrosis A, di Vinci A, Gelvi I, et al. Caspase-8 gene expression in neuroblastoma. Ann N Y Acad Sci 2004;1028:157–67. https://doi.org/10.1196/annals.1322.017. PMID: 15650242.
10. Raman JD, Mongan NP, Tickoo SK, Boorjian SA, Scherr DS, Gudas LJ. Increased expression of the polycomb group gene, EZH2, in transitional cell carcinoma of the bladder. Clin Cancer Res. 2005;11:8570–6. https://doi.org/10.1158/1078-0432.CCR-05-1047.
11. O'Carroll D, Erhardt S, Pagani M, Barton SC, Surani MA, Jenuwein T. The polycomb-group gene Ezh2 is required for early mouse development. Mol Cell Biol 2001;21:4330–6. doi: 10.1128/MCB.21.13.4330-4336.2001. PMID: 11390661.
12. Chamberlain SJ, Yee D, Magnuson T. Polycomb repressive complex 2 is dispensable for maintenance of embryonic stem cell pluripotency. Stem Cells. 2008;26:1496–505. https://doi.org/10.1634/stemcells.2008-0102.
13. Vo BT, Li C, Morgan MA, Theurillat I, Finkelstein D, Wright S, et al. Inactivation of Ezh2 upregulates Gfi1 and drives aggressive Myc-driven group 3 medulloblastoma. Cell Rep. 2017;18:2907–17. https://doi.org/10.1016/j.celrep.2017.02.073.
14. Tsubota S, Kishida S, Shimamura T, Ohira M, Yamashita S, Cao D, et al. PRC2-mediated transcriptomic alterations at the embryonic stage govern tumorigenesis and clinical outcome in MYCN-driven neuroblastoma. Cancer Res. 2017;77:5259–71. https://doi.org/10.1158/0008-5472.CAN-16-3144.
15. Wang C, Liu Z, Woo CW, Li Z, Wang L, Wei JS, et al. EZH2 mediates epigenetic silencing of neuroblastoma suppressor genes CASZ1, CLU, RUNX3, and NGFR. Cancer Res. 2012;72(1):315–24. https://doi.org/10.1158/0008-5472.CAN-11-0961.
16. Bate-Eya LT, Gierman HJ, Ebus ME, Koster J, Caron HN, Versteeg R, et al. Enhancer of Zeste homologue 2 plays an important role in neuroblastoma cell survival independent of its histone methyltransferase activity. Eur J Cancer. 2017;75:63–72. Epub 2017 Feb 17. PMID: 28214660.
17. Chen L, Alexe G, Dharia NV, Ross L, Iniguez AB, Conway AS, et al. CRISPR-Cas9 screen reveals a MYCN-Amplified neuroblastoma dependency on EZH2. J Clin Invest. 2018;128(1):446–62. Epub 2017 Dec 4. PMID: 29202477.
18. Li Z, Takenobu H, Setyawati AN, Akita N, Haruta M, Satoh S, et al. EZH2 regulates neuroblastoma cell differentiation via NTRK1 promoter epigenetic modifications. Oncogene. 2018;37(20):2714–27. https://doi.org/10.1038/s41388-018-0133-3.
19. Yan J, Ng SB, Tay JL, Lin B, Koh TL, Tan J, et al. EZH2 overexpression in natural killer/T-cell lymphoma confers growth advantage independently of histone methyltransferase activity. Blood. 2013;121:4512–20. https://doi.org/10.1182/blood-2012-08-450494.
20. Knutson SK, Kawano S, Minoshima Y, Warholic NM, Huang KC, Xiao Y, et al. Selective inhibition of EZH2 by EPZ-6438 leads to potent antitumor activity in EZH2-mutant non-Hodgkin lymphoma. Mol Cancer Ther. 2014;13(4):842–54. https://doi.org/10.1158/1535-7163.MCT-13-0773.
21. Kurmasheva RT, Sammons M, Favours E, Wu J, Kurmashev D, Cosmopoulos K, et al. Initial testing (Stage 1) of Tazemetostat (EPZ-6438), a novel EZH2 inhibitor, by the pediatric preclinical testing program. Pediatr Blood Cancer. 2017. https://doi.org/10.1002/pbc.26218.
22. Yan W, Herman JG, Guo M. Epigenome-based personalized medicine in human cancer. Epigenomics. 2016;8(1):119–33. https://doi.org/10.2217/epi.15.84.
23. Gao J, Fosbrook C, Gibson J, Underwood TJ, Gray JC, Walters ZS, Review. Targeting EZH2 in neuroblastoma. Cancer Treat Rev. 2023 Sep:119:102600. https://doi.org/10.1016/j.ctrv.2023.102600. PMID: 37467626.
24. Shaliman D, Takenobu H, Sugino RP, Ohira M, Kamijo T. The PRC2 molecule EED is a target of epigenetic therapy for neuroblastoma. Eur J Cell Biol. 2022;101(3): 151238. https://doi.org/10.1016/j.ejcb.2022.151238.
25. Henrich KO, Bender S, Saadati M, Dreidax D, Gartlgruber M, Shao C, et al. Integrative genome-scale analysis identifies epigenetic mechanisms of transcriptional deregulation in unfavorable neuroblastomas. Cancer Res. 2016;76:5523–37. https://doi.org/10.1158/0008-5472.CAN-15-2507.
26. Sugino RP, Ohira M, Mansai SP, Kamijo T. Comparative epigenomics by machine learning approach for neuroblastoma. BMC Genomics. 2022;23(1): 852. https://doi.org/10.1186/s12864-022-09061-y.
27. Iida N, Okuda Y, Ogasawara O, Yamashita S, Takeshima H, Ushijima T. MACON: a web tool for computing DNA methylation data obtained by the Illumina Infinium Human DNA methylation BeadArray. Epigenomics. 2018;10(3):249–58. https://doi.org/10.2217/epi-2017-0093.
28. Kondo Y, Shen L, Cheng AS, Ahmed S, Boumber Y, Charo C, et al. Gene silencing in cancer by histone H3 lysine 27 trimethylation independent of promoter DNA methylation. Nat Genet. 2008;40(6):741–50. https://doi.org/10.1038/ng.159.
29. Liberzon A, Birger C, Thorvaldsdóttir H, Ghandi M, Mesirov JP, Tamayo P. The Molecular Signatures Database (MSigDB) hallmark gene set collection. Cell Syst. 2015;1(6):417–25. doi: 10.1016/j.cels.2015.12.004. PMID: 26771021.
30. Bitler BG, Aird KM, Garipov A, Li H, Amatangelo M, Kossenkov AV, et al. Synthetic lethality by targeting EZH2 methyltransferase activity in ARID1A-mutated cancers. Nat Med. 2015;21(3):231–8. https://doi.org/10.1038/nm.3799.
31. Zhang S, Xiong H, Yang J, Yuan X. Pan-cancer analysis reveals the multidimensional expression and prognostic and immunologic roles of VSTM2L in cancer. Front Mol Biosci. 2022;8: 792154. https://doi.org/10.3389/fmolb.2021.792154.
32. Kawahara K, Hasegawa T, Hasegawa N, Izumi T, Sato K, Sakamaki T, et al. Truncated GPNMB. A microglial transmembrane protein, serves as a scavenger receptor for oligomeric β-amyloid peptide1-42 in primary type 1 microglia. J Neurochem. 2024;168(7):1317–39. https://doi.org/10.1111/jnc.16078.
33. Suda M, Shimizu I, Katsuumi G, Hsiao CL, Yoshida Y, Matsumoto N, et al. Glycoprotein nonmetastatic melanoma protein B regulates lysosomal integrity and lifespan of senescent cells. Sci Rep. 2022;12(1): 6522. https://doi.org/10.1038/s41598-022-10522-3.
34. Shimoda M, Principe S, Jackson HW, Luga V, Fang H, Molyneux SD, et al. Loss of the timp gene family is sufficient for the acquisition of the CAF-like cell state. Nat Cell Biol. 2014;16(9):889–901. https://doi.org/10.1038/ncb3021.
35. Azuma K, Urano T, Ouchi Y, Inoue S. Glucocorticoid-induced gene tripartite motif-containing 63 (TRIM63) promotes differentiation of osteoblastic cells. Endocr J. 2010;57(5):455–62. https://doi.org/10.1507/endocrj.k09e-290.
36. Momparler RL, Côté S, Momparler LF, Idaghdour Y. Epigenetic therapy of acute myeloid leukemia using 5-aza-2′-deoxycytidine (decitabine) in combination with inhibitors of histone methylation and deacetylation. Clin Epigenetics. 2014;6(1): 19. https://doi.org/10.1186/1868-7083-6-19.
37. Peng D, Kryczek I, Nagarsheth N, Zhao L, Wei S, Wang W, et al. Epigenetic silencing of TH1-type chemokines shapes tumour immunity and immunotherapy. Nature. 2015;527(7577):249–53. https://doi.org/10.1038/nature15520.
38. Zhang Y, Zhou L, Safran H, Borsuk R, Lulla R, Tapinos N, et al. EZH2i EPZ-6438 and HDACi Vorinostat synergize with ONC201/TIC10 to activate integrated stress response, DR5, reduce H3K27 methylation, ClpX and promote apoptosis of multiple tumor types including DIPG. Neoplasia. 2021;23(8):792–810. Epub 2021 Jul 8. PMID: 34246076.
39. Frumm SM, Fan ZP, Ross KN, Duvall JR, Gupta S, VerPlank L, et al. Selective HDAC1/HDAC2 inhibitors induce neuroblastoma differentiation. Chem Biol. 2013;20(5):713–25. https://doi.org/10.1016/j.chembiol.2013.03.020.
40. Seneviratne JA, Ravindrarajah D, Carter DR, Zhai V, Lalwani A, Krishan S, et al. Combined inhibition of histone methyltransferases EZH2 and DOT1L is an effective therapy for neuroblastoma. Cancer Med. 2024;13(21): e70082. https://doi.org/10.1002/cam4.70082.
41. Momparler RL, Doré BT, Momparler LF. Effect of 5-aza-2′-deoxycytidine and retinoic acid on differentiation and c-myc expression in HL-60 myeloid leukemic cells. Cancer Lett. 1990;54(1–2):21–8. https://doi.org/10.1016/0304-3835(90)90086-d.
42. Guan H, Xie L, Klapproth K, Weitzer CD, Wirth T, Ushmorov A. Decitabine represses translocated MYC oncogene in Burkitt lymphoma. J Pathol. 2013;229(5):775–83. https://doi.org/10.1002/path.4164.
43. McCabe MT, Ott HM, Ganji G, Korenchuk S, Thompson C, Van Aller GS, et al. EZH2 Inhibition as a therapeutic strategy for lymphoma with EZH2-activating mutations. Nature. 2012;492(7427):108–12. https://doi.org/10.1038/nature11606. Epub 2012 Oct 10. PMID: 23051747.
44. Li B, Chng WJ. EZH2 abnormalities in lymphoid malignancies: underlying mechanisms and therapeutic implications. J Hematol Oncol. 2019;12(1): 118. https://doi.org/10.1186/s13045-019-0814-6.
45. Kim KH, Roberts CW. Targeting EZH2 in cancer. Nat Med. 2016;22(2):128–34. https://doi.org/10.1038/nm.4036.
46. Preston SEJ, Emond A, Pettersson F, Dupéré-Richer D, Abraham MJ, Riva A, et al. Acquired resistance to EZH2 inhibitor GSK343 promotes the differentiation of human DLBCL cell lines towards an ABC-like phenotype. Mol Cancer Ther. 2022;21(4):511–21. https://doi.org/10.1158/1535-7163.MCT-21-0216.

47. Yamagishi M, Kuze Y, Kobayashi S, Nakashima M, Morishima S, Kawamata T, et al. Mechanisms of action and resistance in histone methylation-targeted therapy. Nature. 2024;627(8002):221–8. https://doi.org/10.1038/s41586-024-07103-x.
48. Chase A, Cross NC. Aberrations of EZH2 in cancer. Clin Cancer Res. 2011;17(9):2613–8. https://doi.org/10.1158/1078-0432.CCR-10-2156.
49. Sashida G, Harada H, Matsui H, Oshima M, Yui M, Harada Y, et al. Ezh2 loss promotes development of myelodysplastic syndrome but attenuates its predisposition to leukaemic transformation. Nat Commun. 2014;5: 4177. https://doi.org/10.1038/ncomms5177.
50. Yang L, Rau R, Goodell MA. DNMT3A in haematological malignancies. Nat Rev Cancer. 2015;15(3):152–65. https://doi.org/10.1038/nrc3895. Epub 2015 Feb 19. PMID: 25693834.
51. Brunetti L, Gundry MC, Goodell MA. DNMT3A in leukemia. Cold Spring Harb Perspect Med. 2017;7(2): a030320. https://doi.org/10.1101/cshperspect.a030320.

Publisher's note